THE ASTRONOMICAL JOURNAL, 115:383–390, 1998 February

TWO CLOSE SEPARATION QUASAR-QUASAR PAIRS IN THE LARGE BRIGHT QUASAR SURVEY[1]

PAUL C. HEWETT
Institute of Astronomy, Madingley Road, Cambridge CB3 0HA, England, UK; phewett@ast.cam.ac.uk
CRAIG B. FOLTZ
Multiple Mirror Telescope Observatory, University of Arizona, Tucson, AZ 85721; cfoltz@as.arizona.edu
MARGARET E. HARDING
Institute of Astronomy, Madingley Road, Cambridge CB3 0HA, England, UK; meh@ast.cam.ac.uk
AND
GERAINT F. LEWIS[2]
Astronomy Program, Department of Earth and Space Sciences, State University of New York at Stony Brook, Stony Brook, NY 11794; gfl@uvastro.phys.uvic.ca
Received 1997 August 18; revised 1997 October 20

ABSTRACT

We present photometric and spectroscopic observations of two close quasar-quasar pairs found in the Large Bright Quasar Survey (LBQS). The two components of the 2153−2056 pair ($z = 1.845$, $\Delta\theta = 7\farcs8$, $B = 17.9$ and 21.3) have the same redshifts within the relatively large uncertainty, $\Delta v_{A-B} = -1100 \pm 1500$ km s^{-1}, of the observations. The quasars are most likely spatially coincident, although the possibility that the pair is the result of gravitational lensing cannot be ruled out. The two components of 1148+0055 ($z = 1.879$, $B = 18.5$ and $z = 1.409$, $B = 21.1$; $\Delta\theta = 3\farcs9$) have disjoint redshifts, and the pair has attracted some attention in the context of gravitational lensing following the independent discovery of the pair by Surdej and collaborators. Four close ($\Delta\theta \leq 10\farcs0$) quasar-quasar pairs have now been discovered in the LBQS, and we discuss the probability of identifying pairs with disjoint redshifts and of locating spatially coincident pairs from the systematic investigation of the well-defined quasar catalog.

Key words: gravitational lensing — quasars: general

1. INTRODUCTION

The frequency and properties of close ($\lesssim 10\farcs0$) pairs of quasars on the sky are of interest in the fields of gravitational lensing, where the number of bona fide lenses remains small (Keeton & Kochanek 1996), and the spatial clustering of quasars on scales $\lesssim 100$ kpc, where the number of such systems is also small (Croom & Shanks 1996). An investigation of the properties of close companions to quasars in the Large Bright Quasar Survey (LBQS; Hewett, Foltz, & Chaffee 1995) has produced four close ($< 10\farcs0$) pairs of quasars to date (Hewett, Harding, & Webster 1992). Investigations of two pairs, 1429−0053 (Hewett et al. 1989) and 1009−0252 (Hewett et al. 1994; Surdej et al. 1993), have already been published. Here we present spectroscopic and photometric observations of the two remaining pairs, 2153−2056 and 1148+0055. The close quasar pair 1148+0055 has independently been discovered by Surdej et al. (1993), but no detailed information has been published for either pair.

Section 2 of this paper presents new spectroscopic and photometric data for each of the latter two quasar pairs. The probability of identifying quasar pairs in the LBQS and comments on the merits of gravitational lens models for the pairs are contained in § 3.

2. OBSERVATIONS

2.1. *Pair Identification*

The brighter images in both the 1148+0055 and 2153−2056 pairs were identified as quasar candidates during the selection phase of the LBQS and confirmed spectroscopically as quasars (Hewett et al. 1991; Morris et al. 1991). Redshifts and magnitudes $z = 1.885$, $B_J = 18.14$ (1148+0055) and $z = 1.849$, $B_J = 17.84$ (2153−2056) are listed in Hewett et al. (1995) with a note indicating that the presence of nearby companion objects results in an overestimate of the quasar magnitudes and an error of up to $3\farcs0$ in the celestial coordinates.

As part of an investigation into the frequency of strong gravitational lenses in the LBQS, all the quasars were inspected visually to provide a census of companion objects within a radius of $10\farcs0$. Film copies of the UK Schmidt Telescope (UKST) B_J direct plates scanned for the LBQS project, or, if available, better quality B_J survey plates, were used and companions to $B_J = 21.5$–22, depending on the quality and depth of the B_J survey plate, were identified. In practice, the physical extent of the high-density images of the relatively bright LBQS quasars on the B_J survey plates precludes the detection of faint companions closer than $\sim 3\farcs0$. Quasar 1148+0055 was noted as possessing a faint stellar companion with a separation of $\sim 4\farcs0$, and 2153−2056 a companion with a separation of $\sim 7\farcs5$.

2.2. *2153−2056: Spectroscopy*

Follow-up spectroscopy of both components of the 2153−2056 pair was obtained at the Anglo-Australian Telescope (AAT) on 1989 August 29. Observations were made with the RGO spectrograph and 25 cm camera,

[1] Some of the observations reported here were obtained with the Multiple Mirror Telescope, a joint facility of the Smithsonian Institution and the University of Arizona.

[2] Current address: Department of Astronomy, University of Washington, Box 351580, Seattle, WA 98195-1580; and Department of Physics and Astronomy, University of Victoria, P.O. Box 3055, Victoria, BC V8W 3P6, Canada.

employing a 600 groove mm^{-1} grating, and the Image Photon Counting System as the detector. Three exposures, 2500 and 2 × 3600 s, were obtained. The slit width was 1.″8 and the slit was oriented at P.A. = 152° across both members of the pair. The spectrograph configuration, slit width, and detector combination yielded a wavelength resolution of ∼8 Å and a usable wavelength coverage of ∼3800–5800 Å. The spatial scale along the slit was 0.″4 $pixel^{-1}$. Atmospheric transmission and the seeing, ∼1.″0, were both good throughout the period of the observations.

Data reduction was performed using standard procedures available in the Starlink FIGARO spectroscopic reduction package. The primary and secondary spectra are well separated on the detector, and no particular difficulties were encountered during the reduction. A flat field was obtained from an exposure of a tungsten lamp, and wavelength calibration was based on exposures of a CuAr arc lamp before and after the observations of 2153−2056. A standard atmospheric extinction correction was applied to the spectra, but, given the low signal-to-noise ratio of the companion spectra, no attempt to perform absolute or relative flux determination was made. Following the extraction of the one-dimensional, extinction-corrected spectra from the individual frames, the spectra were summed to produce the spectra shown in Figure 1.

Compared with the discovery spectrum (Morris et al. 1991), the AAT spectrum of the LBQS quasar has more limited wavelength coverage but a higher signal-to-noise ratio. The two spectra are consistent, and the quasar is an unremarkable representative of the class of optically selected quasars. The redshift derived from the AAT spectrum via cross-correlation with a composite spectrum (Francis et al. 1991) is $z = 1.845 \pm 0.003$, compared with $z = 1.849 \pm 0.005$ reported in Hewett et al. (1995) based on the discovery spectrum.

The spectrum of the companion object (B) has poor signal-to-noise ratio, but the presence of broad emission features at ∼4400 and ∼5400 Å makes its identification as a quasar with $z \sim 1.85$ unambiguous. Scaling the spectrum of the LBQS quasar (A) to the same mean count level over the wavelength range 4250–5500 Å confirms that the fainter object has a very similar overall continuum shape and comparable emission-line properties. A cross-correlation of the two spectra produces a velocity difference $\Delta v_{A-B} = -1100 \pm 1500$ km s^{-1}, with the spectrum of B redshifted relative to that of A. The spectra are thus consistent with both components' lying at the same redshift, but with a rather large uncertainty.

The most obvious difference between the two spectra is the extended depression in the continuum of the B component centered at ∼4230 Å. The feature is visible in the individual sky-subtracted two-dimensional frames and is certainly real. The characteristics of the absorption are typical of a C IV λ1550 broad absorption line (BAL) trough with a peak ejection velocity of ∼18,000 km s^{-1}. This interpretation is reinforced by the apparent turndown at ∼3950 Å in the spectrum of *B*, which is consistent with the presence of an Si IV λ1400 BAL trough.

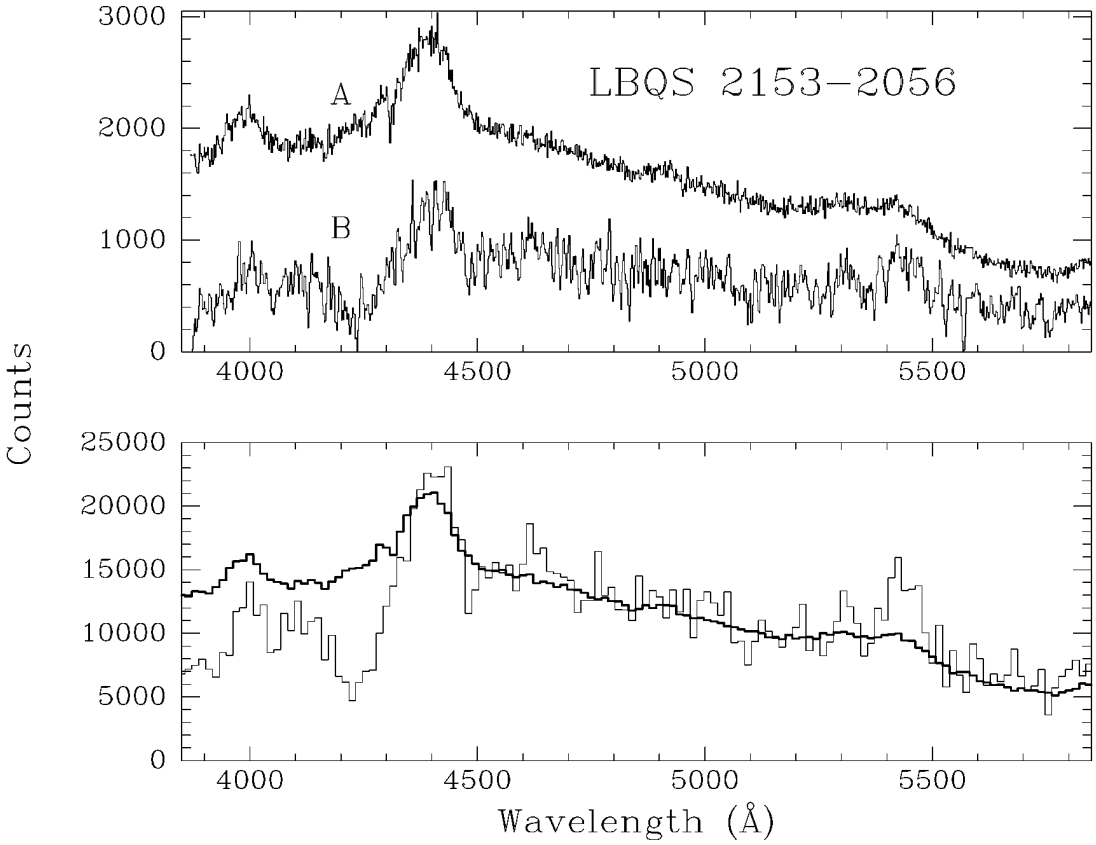

FIG. 1.—*Top*: AAT + RGO spectrograph spectra of LBQS 2153−2056A,B. No flux calibration has been applied, and for the purpose of this figure, the data for component B have been multiplied by a factor of 15 and smoothed with a 3 pixel–wide running boxcar. Note the presence of a clear C IV broad absorption trough in the spectrum of B centered at about 4250 Å. *Bottom*: Uncalibrated spectra binned into 15 Å pixels and overplotted. Note that, longward of 4500 Å, the two spectra are similar to one another; shortward of 4500 Å, the spectrum of B is affected by strong broad absorption.

The spectrum of the A component shows weak absorption features at 4308.3 and 4316.2 Å; the ratio of the wavelengths is 1.00183, close to the 1.00166 for the C IV $\lambda\lambda$1548.2, 1550.8 doublet. The probable identification is with a C IV doublet at $z = 1.783$ and rest equivalent width ~ 0.7 Å.

2.3. *2153−2056: Photometry*

Optical *BVRI* magnitudes were obtained using the 2.5 m Isaac Newton Telescope (INT) on La Palma on 1989 September 5 (*R* and *I*) and September 8 (*B* and *V*). An RCA CCD with 30 μm pixels, yielding an image scale of 0.″74 pixel^{-1}, was employed as the detector. KPNO filters were used with observations of standards taken from Christian et al. (1985). Bias frames were obtained during both nights, while flat fields were derived from twilight sky exposures. Observations of standards at the beginning and end of the nights, and at intervals throughout, were obtained to allow determination of the extinction and color transformations. Observations of 2153−2056 were obtained at air mass 1.5–1.6. Transparency was good on both nights and the seeing was excellent, although the FWHM of images measured from CCD frames of the quasar pair was limited by the large pixels to $\sim$1.″4. Exposure times were 3 × 200 s (*B*), 3 × 200 s (*V*), 8 × 300 s (*R*), and 2 × 300 s (*I*).

Data reduction was performed using standard procedures within IRAF.[3] Magnitudes were derived using M. J. Irwin's IMAGES software (Irwin & Hall 1982; Irwin 1985). Extinction, zero points, and color transformations were well determined. The errors of some of the standard magnitudes from Christian et al. (1985) are substantial, but the residuals of the standards about the derived fits are consistent with a contribution to the rms scatter from the CCD observations of $\lesssim$0.02 mag. The resulting Johnson *BV* magnitudes and Kron-Cousins *RI* magnitudes are given in Table 1. The quoted errors include uncertainties in the zero-point determination and color transformations.

The B1950.0 coordinates of the A component derived by matching stars visible on the CCD frames to the corresponding images in the Automatic Plate Measuring Facility (APM) scan of the UKST plate are ($21^h53^m06^s.57$, $-20°56'03''.1$), approximately 0.″9 southeast of the position quoted by Hewett et al. (1995). This difference is consistent with the bias induced by the presence of the faint companion, which is merged with the brighter component in the APM scan. The separation of the two components derived from the *V* and *R* frames is $\Delta\theta = 7''.8 \pm 0''.1$, and the position angle of the fainter component relative to the brighter component is P.A. = 331° ± 2°. Figure 2 shows a 134.″0 × 134.″0 region centered on the A component of the pair from the co-added *R*-band CCD frame.

The CCD frames have 1 σ sky fluctuations within a 4.″4 diameter aperture of 24.6, 24.3, and 25.1 mag for the *B*, *V*, and *R* frames, respectively. There is no evidence for the presence of any additional images, apart from the B component of the pair, within a 15.″0 radius of component A. However, the very large pixels preclude the detection of faint images close to component A via point-spread function subtraction techniques, and it is not possible to rule out the presence of an image fainter than $R \sim 22.0$ within 1.″5 of component A.

The number counts in the field turn over at $R \sim 24.0$, and the image catalog appears to be largely complete to $R = 23.8$. There are 293 images with magnitudes $21.0 \leq R \leq 23.8$ in an area of 0.0067 deg^2. Reliable image classification is not possible for the fainter objects, but the CCD frame, which is at Galactic coordinates (l, b) = (32°, −50°), contains significantly more stars than a typical high-latitude field. The *R*-band galaxy counts of Metcalfe et al. (1995) predict 243 galaxies with magnitudes $21.0 \leq R \leq 23.8$ in an area of 0.0067 deg^2. Allowing for the presence of stars in the image catalog, the galaxy number counts are in excellent agreement and there is no evidence of a significant excess. The spatial distribution of objects over the frame is uniform on large scales, with fluctuations evident on scales of 30.″0–60.″0. The quasar pair lies in a region that is somewhat underdense relative to the mean.

Infrared JHK_n magnitudes were obtained using the IRIS spectrograph at the AAT on 1992 October 13. A 128 × 128 Rockwell HgCdTe array with 60 μm pixels, producing an image scale of 0.″6 pixel^{-1}, was employed as the detector. The 2153−2056 pair was observed in *H* and K_n using a five-point dither with an offset of 10.″0 in right ascension

[3] IRAF is distributed by the National Optical Astronomy Observatories, which are operated by the Association of Universities for Research in Astronomy, Inc., under cooperative agreement with the National Science Foundation.

TABLE 1

PHOTOMETRIC OBSERVATIONS

Component	*B*	*V*	*R*	*I*	*J*	*H*	*K*
2153−2056A:							
1989 Sep 5	...	...	17.28 ± 0.03	16.78 ± 0.03	...	...	...
1989 Sep 8	17.93 ± 0.03	17.51 ± 0.03	...	...	...	...	...
1992 Oct 13	...	...	...	...	16.60 ± 0.05	16.28 ± 0.08	15.65 ± 0.09[a]
1993 Sep 10	...	...	17.53 ± 0.05	17.35 ± 0.05	...	...	...
2153−2056B:							
1989 Sep 5	...	...	20.43 ± 0.05	19.69 ± 0.05	...	...	...
1989 Sep 8	21.26 ± 0.05	20.64 ± 0.05	...	...	...	...	...
1148+0055A:							
1992 Apr 1	18.48 ± 0.03	18.16 ± 0.03	...	...	...	...	...
1994 Feb 24.....	...	...	...	...	16.91 ± 0.05	16.43 ± 0.05	15.80 ± 0.05
1994 May 2	...	18.19 ± 0.03	17.88 ± 0.03	...	...	...	...
1148+0055B:							
1992 Apr 1	21.13 ± 0.09	21.07 ± 0.08	...	...	...	...	...
1994 Feb 24.....	...	...	...	...	20.1 ± 0.2	19.4 ± 0.3	18.3 ± 0.2
1994 May 2	...	21.22 ± 0.15	20.90 ± 0.12	...	...	...	...

[a] The *K* observations for the two pairs used different filters; the entry for 2153−2056A is a K_n magnitude.

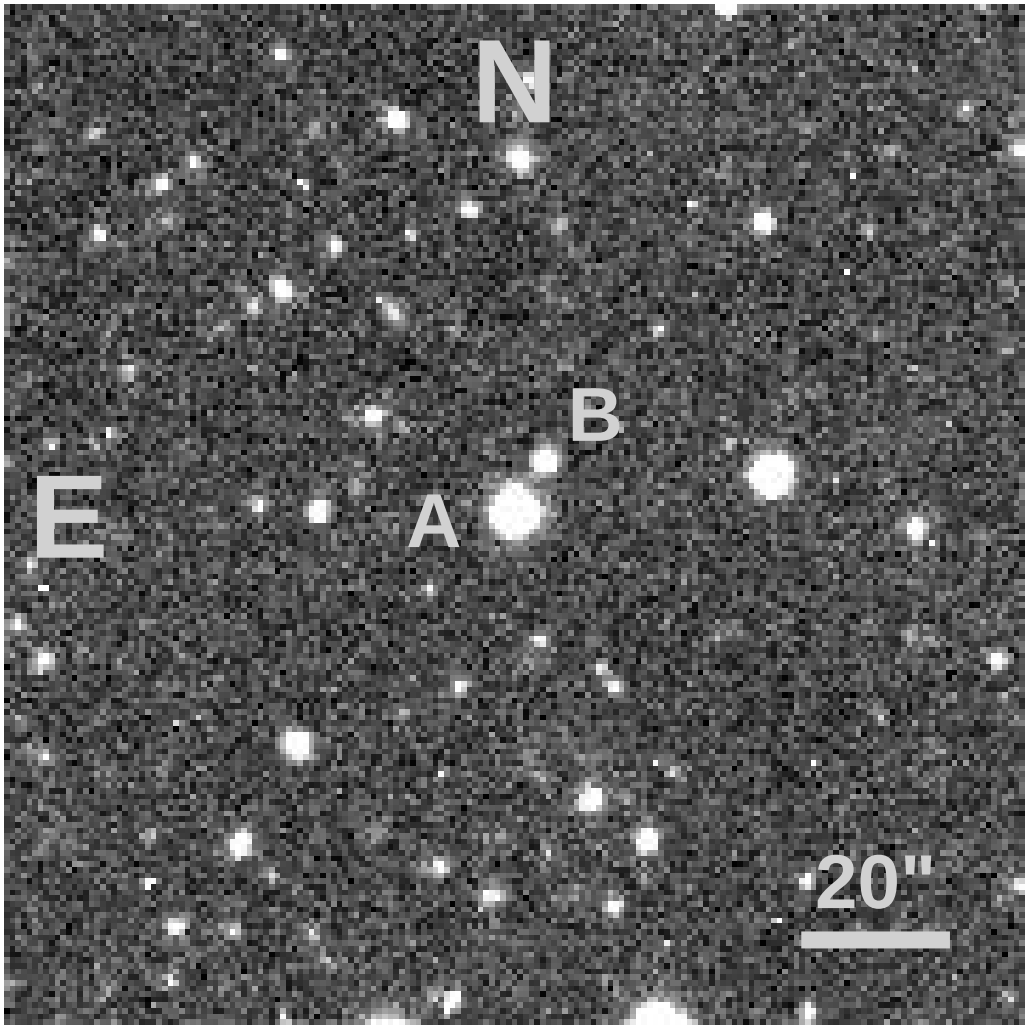

FIG. 2.—*R*-band CCD image of a 134″.0 × 134″.0 region centered on the A component of the quasar pair 2153−2056. North is to the top, with east to the left. The quasar components are indicated by the labels "A" and "B."

and declination between positions. Exposure times were 125 s per position, yielding total exposure times of 600 s in both H and K_n. A two-position, 25″.0 separation, 125 s exposure strategy was adopted for the J observations to obtain a total exposure time of 250 s per target. The K_n filter has a narrower FWHM, extending over the range 2.0–2.3 μm, and lower effective wavelength in comparison with the conventional K filter. A transmission curve for the K_n filter can be found in the IRIS Users' Guide (Allen 1993).

All frames were first linearized and dark-subtracted using a standard procedure (Allen 1993). Subsequent data reduction was accomplished using IRAF routines. A normalized flat field, derived separately for each filter, from exposures of an illuminated dome screen at the start of the night, was divided into all the object exposures. Sky frames were then generated by combining groups of dithered object exposures. A scaled version of the sky frame was subtracted from each object frame, and the resulting sky-subtracted object frames were combined using integer pixel shifts in the spatial registration procedure and a mask to ensure the small number of bad pixels in the array did not contribute to the final summed image. SAAO standards (Carter & Meadows 1995) were observed throughout the night to provide zero points (on the SAAO system) and extinction values. Magnitudes were derived using the IMAGES software and are given in Table 1. The quoted errors include uncertainties in the zero-point determination.

The fainter B component of the pair is just visible in all three bands, but the flux excess in a 3″.6 diameter aperture is only 2–3 σ of the sky background fluctuations. Relative photometry of both members of the pair using a 3″.6 aperture yields magnitudes for the companion of $J = 20.5 \pm 1.0$, $H = 19.2 \pm 0.5$, and $K_n = 18.3 \pm 0.4$. A composite frame, made from averaging the J, H, and K_n frames, produces a relative magnitude difference between the components of $\Delta m_{B-A} = 3.3 \pm 0.3$. Thus, within the very poor constraints, the optical to infrared colors of both components are similar. No other images are visible in the infrared frames within a radius of 30″.0 of the A component.

2.4. *1148+0055: Spectroscopy*

Follow-up spectroscopy of both components of the 1148+0055 pair was obtained at the Multiple Mirror Telescope (MMT) on 1990 June 17. The Red Channel of the MMT spectrograph was used with a 150 groove mm^{-1} grating and a thinned Texas Instruments 800 × 800 pixel CCD as the detector. One exposure of 1200 s duration was obtained. The slit width was 1″.25, and the slit was oriented

at P.A. = 105° across both primary and secondary members of the pair. The spectrograph configuration, slit width, and detector combination yielded a wavelength resolution of ~20 Å and a usable wavelength coverage of ~3200–7750 Å. The spatial scale along the slit was 0.″6 pixel^{-1}. Atmospheric transmission and the seeing, ~1.″0, were both good throughout the period of the observations.

Data reduction was performed using standard IRAF procedures. The primary and secondary spectra were well separated on the detector, and no particular difficulties were encountered during the reduction. A flat field was obtained from an exposure of a quartz lamp, and wavelength calibration was based on exposures of an HeNeAr arc lamp taken after the observation of 1148+0055. A standard atmospheric extinction correction was applied to the spectra. The observations were flux-calibrated using observations of standard stars, but no attempt to determine absolute fluxes was made.

The observations were taken at an air mass of 1.8, the slit was not aligned at the parallactic angle, and the MMT's intensified television camera is sensitive primarily to red wavelengths. Thus, notwithstanding the flux calibration procedure, the quasar spectra show a significant loss of light shortward of about 4500 Å due to the effects of atmospheric dispersion. To correct for the systematic loss of flux, the spectra were first divided by the composite spectrum of Francis et al. (1991), the continuum flux distribution of which is similar to that of the LBQS quasar 1148+0055 (Hewett et al. 1991). A low-order polynomial was fitted to the result and divided into the original spectra to produce the spectra shown in Figure 3. The shape of the corrected spectrum of 1148+0055 and the original discovery spectrum are in good agreement, and the relative fluxes should be accurate to ~20% or better.

The redshift of the LBQS quasar, component A, derived via cross-correlation with the LBQS composite spectrum is $z = 1.879 \pm 0.003$, compared with $z = 1.885 \pm 0.005$ reported by Hewett et al. (1995), based on the discovery spectrum. The emission-line and continuum properties are not at all unusual for an optically selected quasar.

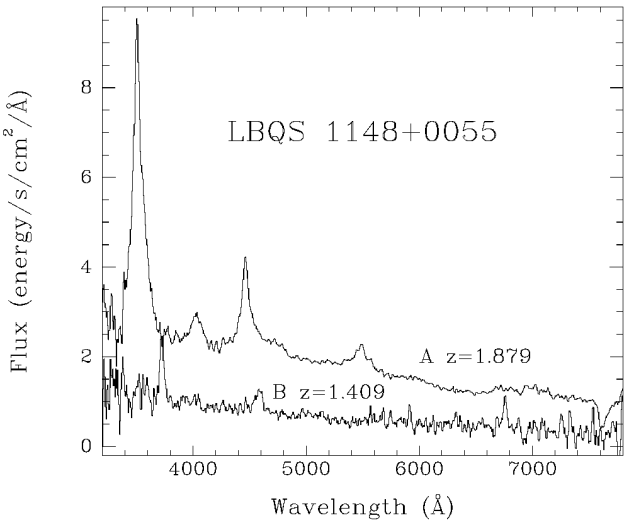

FIG. 3.—MMT Red Channel spectra of LBQS 1148+0055A,B. For the purpose of this figure, the data for component B have been multiplied by a factor of 3 and smoothed with a 3 pixel–wide running boxcar. The continuum shapes of the spectra have been adjusted to that of the LBQS composite spectrum (see text for details).

The spectrum of the B component shows strong broad emission at roughly 3730, 4580, and 6750 Å, and combined with the presence of an extended continuum, identification as a quasar with $z \sim 1.4$ exhibiting C IV λ1550, C III] λ1909, and Mg II λ2798 emission lines is unambiguous. The cross-correlation redshift is $z = 1.409 \pm 0.003$. Within the constraints of the relatively poor signal-to-noise ratio, there is nothing remarkable about the spectrum.

The spectrum of the A component was searched for absorption arising in, or associated with, the lower redshift B component. At a redshift of $z = 1.409$, C IV $\lambda\lambda$1548, 1550 and Mg II $\lambda\lambda$2796, 2803 doublets at about 3734 and 6745 Å fall within the wavelength coverage of the spectrum of the A component. No significant features were seen. Given the relatively low spectral resolution and signal-to-noise ratio of the spectrum, the rest equivalent width limit on an unresolved absorption line is a relatively large 3 Å, and a higher quality spectrum is necessary for absorption-line detections or to establish interesting upper limits.

2.5. *1148+0055: Photometry*

Optical *BVR* magnitudes were obtained using the 1 m Jacobus Kapteyn Telescope (JKT) on La Palma on 1992 April 1 (*B* and *V*) and 1994 May 2 (*V* and *R*). In 1992, a GEC CCD with 22.0 μm pixels, yielding an image scale of 0.″30 pixel^{-1}, was employed as the detector.[4] KPNO filters were used with observations of standards taken from Landolt (1983). In 1994, an EEV CCD with 22.5 μm pixels, yielding an image scale of 0.″31 pixel^{-1}, was employed as the detector. Harris filters were used with observations of standards taken from Landolt (1992). Bias frames were obtained during both nights and flat fields were derived from twilight sky exposures. Observations of standards at the beginning and end of the nights, and at intervals throughout, were obtained to allow determination of the extinction and color transformations. Observations of 1148+0055 were obtained at low air mass, $\lesssim$1.2, and transparency was good on both nights, although in 1992 there was a small systematic variation in the vertical extinction of 0.007 $\pm$ 0.001 mag hr^{-1}. The FWHMs of images measured from CCD frames of the quasar pair were $\lesssim$1.″0. Exposure times were 2 × 500 s (*V*) and 2 × 1000 s (*B*) in 1992 and 2 × 500 s (*V*) and 2 × 500 s (*R*) in 1994.

Data reduction was performed using standard procedures within IRAF. Magnitudes were derived using M. J. Irwin's IMAGES software. Extinction, zero points, and color transformations were well determined, with residuals of the standards about the derived fits typically $\lesssim$0.02 mag. The resulting Johnson *BV* magnitudes and Kron-Cousins *R* magnitude are given in Table 1. The quoted errors include uncertainties in the zero-point determination and color transformations. The *R* magnitudes of the components are in good agreement with those published by Surdej et al. (1993).

The B1950.0 coordinates of the A component derived by matching stars visible on the CCD frames to the corre-

[4] The CCD employed on this night was incorrectly identified as an EEV 1242 × 1152 pixel CCD in Hewett et al. (1994). Although the correct image scale was employed to calculate the separation of the images in the 1009−0252 system, the relative separations of component B from A listed in Table 1 of that paper should read (−0.61, −1.41), in agreement with the legend to Fig. 1 of Hewett et al. (1994). This inconsistency has previously been noted by Keeton & Kochanek (1996).

sponding images in the APM scan of the UKST plate are within 0.″1 of the position quoted by Hewett et al. (1995), i.e., ($11^h48^m41^s.56$, $+00°55'07''.8$). The presence of the faint companion, which is merged with the brighter component in the APM scan, had essentially no effect on the centroid position of the brighter component. The separation of the two components derived from the B, V, and R frames is $\Delta\theta = 3''.9 \pm 0''.1$, and the position angle of the fainter component relative to the brighter component is P.A. $= 111° \pm 2°$. The separation of the components is in excellent agreement with that published by Surdej et al. (1993).

The CCD frames are not particularly deep, with 1 σ sky fluctuations within a 3.″6 diameter aperture of 24.0, 23.5, and 23.2 mag for the B, V, and R frames, respectively. There are a number of faint galaxies ($V \sim 22.5$, $R \sim 21$) within the annulus 20.″0–60.″0 from the pair, but there is no significant enhancement of images or otherwise unusual feature of the immediate ($\sim 1'.0$) neighborhood. The closest object to the pair, $\sim 18''$ distant and P.A. $\sim 304°$ from component A, is compact with magnitudes $R = 20.9 \pm 0.2$ and $V = 22.7 \pm 0.3$. Figure 4 shows a 134.″0 × 134.″0 region centered on the A component of the pair from the co-added R-band CCD frame.

Infrared JHK magnitudes were obtained using the UK Infrared Telescope (UKIRT) on 1994 February 24. A 58 × 62 Santa Barbara Research Corporation InSb array with 15 μm pixels, producing an image scale of 0.″6 pixel^{-1}, was employed as the detector. The 1148+0055 pair was observed in each band using a five-point dither with an offset of 8.″0 in right ascension and declination between positions. Transparency was good and the seeing was excellent, although the FWHM of images measured from CCD frames of the quasar pair was limited by the size of the detector pixels to $\sim 1''.1$. Exposure times were 120, 80, and 90 s per position, yielding total exposure times of 600, 400, and 450 s in J, H, and K, respectively. Data reduction was accomplished using IRAF routines and involved subtraction of a dark frame from each exposure, followed by combination of the dithered object exposures to produce a flat-field frame. A normalized version of the flat field was then divided into each object frame. The resulting object frames were combined using integer pixel shifts in the spatial registration procedure and a mask to ensure the small number of bad pixels were excluded from the final summed image. Standards from the UKIRT bright-standard list were observed throughout the night to provide zero points (on the UKIRT system) and extinction values. Magnitudes for the bright member of the pair were derived using IMAGES and are given in Table 1. The quoted errors include uncertainties in the zero-point determination.

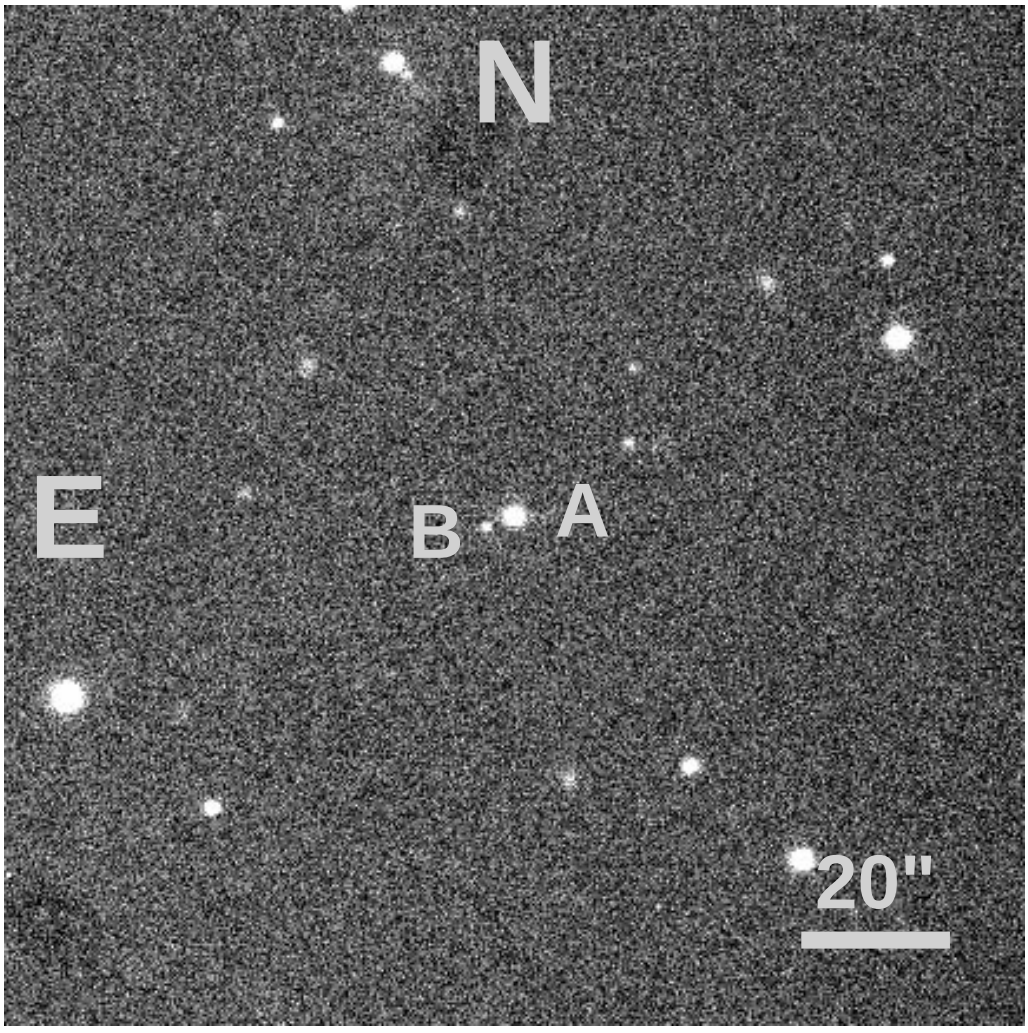

FIG. 4.—Same as Fig. 2, but for 1148+0055

The fainter B component of the pair is present in all three bands at 5–7 σ of the sky background fluctuations. Relative photometry of both members of the pair using a 3.″6 diameter aperture was employed to derive the magnitudes for the companion given in Table 1. The overall optical to infrared colors of both components are similar. The infrared colors of the B component appear to be significantly redder than those of the A component, although the errors are substantial.

There is one other object visible within the small 22.″0 × 20.″0 area of the *JHK* frames. The object is 5.″0 ± 0.″2 from A at P.A. = 276° ± 2°, placing it almost opposite component B. The object is well detected in the *J* and *K* frames but barely present in the *H* frame. Magnitudes, derived using differential photometry in a 3.″6 diameter aperture relative to component A, are $J = 20.4 \pm 0.2$, $H = 21.2 \pm 1.0$, and $K = 18.4 \pm 0.2$. Inspection of the *R*-band CCD frame reveals a suggestion of something coincident with the infrared detection but far too faint to perform any form of photometry.

Taking a *K*-band detection limit in the UKIRT infrared frames of $K = 19.0$, the predicted surface density of galaxies within a radius of $\Delta\theta = 10.''0$ from the LBQS component of 1148+0055 is ∼0.4, where the galaxy surface density is taken from McLeod et al. (1995). The detection of one such object is thus not unexpected. The photometric data are poor but the *K* magnitude, $J-H$ color, and the limit to the optical to infrared color are consistent with identification as a luminous, L^*, early-type galaxy at redshift $z \sim 1$ (see magnitude and color predictions in McLeod & Rieke 1995 and Songaila et al. 1994). However, much higher quality optical and infrared photometry, or a spectroscopic redshift, is required to classify the object.

3. DISCUSSION

The discovery of close quasar-quasar pairs with discordant redshifts has stimulated considerable interest. Specifically, the quasar-quasar pair 1148+0055, along with the 1009−0252 pair (Hewett et al. 1994), has been discussed in the context of weak gravitational lensing (Burbidge, Hoyle, & Schneider 1997; Wampler 1997), although it has not been appreciated that both pairs were discovered among a well-defined sample of quasars, i.e., the LBQS. The selection effects that determine the probability of locating close ($\lesssim 10.''0$) pairs of objects in the LBQS are not simple, and the spectroscopic follow-up of the large number of faint objects around the 1055 LBQS quasars is a nontrivial undertaking. Consequently, the definitive analysis of the frequency and properties of quasar-quasar and quasar-galaxy pairs in the LBQS is not yet available. However, it is possible to perform a reliable a priori calculation of the number of companion quasars expected by chance to be found within an annulus, $3.''0 \le \theta \le 10.''0$, about all of the 1055 LBQS quasars The search for companion quasars performed on the entire LBQS catalog is sensitive to companions with magnitudes $B_J \le 21.5$, redshifts $0.2 \le z \le 3.4$, and separations $3.''0 \le \theta \le 10.''0$. The surface density of such quasars to $B_J = 21.5$ is ∼70 deg^{-2} (Hartwick & Schade 1990) and the total area surveyed is 0.0233 deg^2, yielding a predicted number of 1.6 unrelated quasar-quasar pairs within the LBQS. The follow-up spectroscopy of viable candidates for companion quasars is almost complete; the efficiency of the identifications within the specified magnitude and separation limits is close to 100%, and it is unlikely that further pairs will be identified. Thus, the detection of two quasar-quasar pairs in the survey is not unexpected. This conclusion is at variance with that reached by Burbidge et al. (1997). The difference is attributable to a combination of factors, including the values taken by Burbidge et al. for the number of quasars surveyed (648 vs. 1055), the smaller maximum separation limit ($\theta < 5.''0$ vs. $3.''0 \le \theta \le 10.''0$), and the brighter quasar magnitude limits ($m \le 19.3$ and $m \le 20.7$ vs. $B_J \le 21.5$). It is true that both the quasar-quasar pairs discovered in the LBQS have separations $\theta < 5.''0$ and that one of the companion quasars is relatively bright. However, the frequency of quasar-quasar pairs found in the LBQS is consistent with the a priori calculation based on the well-defined survey parameters.

The rather high probability of finding close pairs of quasars with discordant redshifts in the LBQS catalog by chance does not mean that gravitational lensing of quasars by mass associated with foreground quasars is unimportant; Wampler (1997) reviews the lensing hypothesis. If the unidentified object detected in the infrared frames is a high-redshift ($z \sim 1$), massive, early-type galaxy, its effect, combined with that of the mass associated with the low-redshift quasar, could produce a magnification of the LBQS quasar. However, the magnification is not expected to be very large, $\lesssim 0.5$ mag, as there is no evidence of multiple images and the cross section for an isothermal deflector producing a magnification as large as 2 is very small.

The 2153−2056 pair ($z = 1.85$, $\Delta\theta = 7.''8$, $B = 17.9$ and 21.3) has a number of similarities to the 1429−0053 pair ($z = 2.08$, $\Delta\theta = 5.''1$, $B = 17.7$ and 20.8; Hewett et al. 1989) also found in the LBQS catalog. Such pairs may arise as a result of the spatial clustering of quasars (Croom & Shanks 1996) or from strong gravitational lensing by a massive ($> 10^{12}\ M_\odot$) intervening object.

At $z = 2.0$, $1.''0 \simeq 5\ h^{-1}$ kpc for cosmologies with $\Omega = 0.3$–1 and zero cosmological constant.[5] Little is known about the clustering properties of quasars on the small spatial scales, $\lesssim 50\ h^{-1}$ kpc, corresponding to the $\lesssim 10.''0$ separations of the LBQS quasar-quasar pair data. Extrapolating the observationally determined properties of quasar clustering on megaparsec scales, where the spatial two-point correlation function at separation $r\ h^{-1}$ Mpc is $\xi \sim (r/r_0)^{-1.8}$, $r_0 = 6\ h^{-1}$ Mpc (Croom & Shanks 1996), produces an excess of 4 orders of magnitude in the number of quasars expected within $50\ h^{-1}$ kpc of a quasar, relative to that expected for an unclustered population. The faint apparent magnitude limit probed, $B_J \sim 21.5$, means companion objects well down the luminosity function can be detected ($M_{B_J} \sim -23.8$ at $z = 2.0$ for $h = 0.5$ and $\Omega = 1$) and the spatial density is relatively high, $\sim 10^{-6}$ quasars Mpc^{-3}. However, as stressed by Djorgovski (1991), even the high spatial density coupled with the enhanced probability of finding a quasar within $\lesssim 100\ h^{-1}$ kpc falls several orders of magnitude short of explaining the number of common-redshift close pairs found in various quasar surveys. The statistics for the LBQS survey confirm the conclusions of Djorgovski (1991), with only ∼0.01 quasar pairs predicted compared with the two observed. As noted in that study, there is no reason why a simple extrapolation of the clustering behavior evident at large separations in the linear regime should be valid at close separations, where several additional physical processes may be important,

[5] Where h is the Hubble constant in units of 100 km s^{-1} Mpc^{-1}.

including the possibility of close encounters triggering enhanced fueling of active galactic nuclei. The very large surveys, ~20,000 quasars, planned for the Anglo-Australian Telescope's 2dF multifiber instrument should place the empirically determined behavior of quasar clustering on small scales ($\lesssim 1\ h^{-1}$ Mpc) on a much firmer footing, thereby allowing a much improved assessment of whether the number of detected quasar-quasar pairs at very small scales, $\lesssim 100\ h^{-1}$ kpc, is consistent with the spatial clustering of quasars.

Under the gravitational lensing hypothesis, only the separation of the 2153−2056 quasar pair and their relative fluxes[6] provide constraints on the model. Assuming the deflector can be modified as a singular isothermal sphere (Schneider, Ehlers, & Falco 1992) and lies at a redshift $z = 1.0$, the gravitational lensing solution is determined exactly. The velocity dispersion of the deflector is $\sigma_v \sim 690$ km s^{-1}, equivalent to that of an Abell richness class 1 cluster (Zabludoff, Huchra, & Geller 1990). The centroid of the deflector lies between the two quasars, ~7.″4 away from the brighter system. The ability to detect a relatively poor Abell cluster at $z \gtrsim 1$ with images of the depth of the INT R-band frame is poor (Postman et al. 1996), and the photometric data are consistent with the presence of such a cluster but offer no positive evidence to support the lensing hypothesis. The most probable redshift for a deflector is $z_d \sim 0.6$, significantly lower than the $z_d = 1.0$ employed above, reducing the velocity dispersion of the deflector to ~520 km s^{-1}, but the lack of any evidence for an overdensity of galaxies arising from the presence of a cluster at $z \sim 0.6$ mitigates against such a geometry and offers no evidence in favor of the lensing hypothesis.

Macrolensed BAL quasars can provide a valuable insight on the nature of the absorbing material. In the case of 2153−2056, the path separation to the two images is $\sim 5 \times 10^{15}$ cm for a BAL region 200 pc from the quasar core. The time delay between the images from the model with a deflector at $z_d = 1.0$ is $\sim 16\ h^{-1}$ yr. This value is reasonably insensitive to cosmology, and such a time delay, coupled with intrinsic variability of the quasar source, could conceivably account for the observed spectral differences between the images.

Considering individual systems it is difficult to rule out the lensing hypothesis completely; however, under the lensing hypothesis it is predicted that lensed image pairs with similar flux ratios should be more prevalent than image pairs with more disparate fluxes (Kochanek 1995). The selection of the 1429−0053 and 2153−2056 pairs with their large brightness ratios, without the detection in the LBQS of a larger number of quasar pairs with more similar fluxes, argues against the lensing hypothesis for the origin of the pairs.

The LBQS is supported by National Science Foundation grants AST 90-01181 and 93-20715. The LBQS would not have been possible without the active support of the United Kingdom Schmidt Telescope Unit and the staff of the Automated Plate Measuring Facility. We are grateful to the referee, Chris Kochanek, for highlighting the difference between the predicted and observed flux ratios of the quasar pairs under the lensing hypothesis. The authors acknowledge the data analysis facilities provided by the Starlink Project, which is run by CCLRC on behalf of PPARC. A NATO Collaborative Research Grant aids research on gravitational lenses and quasar surveys at the Institute of Astronomy. The INT and JKT are operated on the island of La Palma on behalf of PPARC and NWO at the Observatorio del Roque de los Muchachos of the Instituto de Astrofísica de Canarias. Telescope operators at the AAT, MMT, and La Palma provided valuable support, and we would also like to thank Rachel Webster, who helped obtain the spectra of 2153−2056 at the AAT.

[6] Any possible microlensing-induced magnification due to the action of individual stars in a lensing galaxy has been neglected.

REFERENCES

Allen, D. A. 1993, IRIS Users' Guide (AAO User Manual 30a) (vers. 2.5; Epping: AAO)
Burbidge, G., Hoyle, F., & Schneider, P. 1997, A&A, 320, 8
Carter, B. S., & Meadows, V. S. 1995, MNRAS, 276, 734
Christian, C. A., Adams, M., Barnes, J. V., Butcher, H., Hayes, D. S., Mould, J. R., & Siegal, M. 1985, PASP, 97, 363
Croom, S. M., & Shanks, T. 1996, MNRAS, 281, 893
Djorgovski, S. 1991, in ASP Conf. Ser. 21, The Space Distribution of Quasars, ed. D. Crampton (San Francisco: ASP), 349
Francis, P. J., Hewett, P. C., Foltz, C. B., Chaffee, F. H., Weymann, R. J., & Morris, S. L. 1991, ApJ, 373, 465
Hartwick, F. D. A., & Schade, D. 1990, ARA&A, 28, 437
Hewett, P. C., Foltz, C. B., & Chaffee, F. H. 1995, AJ, 109, 1498
Hewett, P. C., Foltz, C. B., Chaffee, F. H., Francis, P. J., Weymann, R. J., Morris, S. L., Anderson, S. F., & MacAlpine, G. M. 1991, AJ, 101, 1121
Hewett, P. C., Harding, M. E., & Webster, R. L. 1992, in Lecture Notes in Physics, 406, Gravitational Lenses, ed. R. Kayser, T. Schramm, & L. Neiser (Berlin: Springer), 209
Hewett, P. C., Irwin, M. J., Foltz, C. B., Harding, M. E., Corrigan, R. T., Webster, R. L., & Dinshaw, N. 1994, AJ, 108, 1534
Hewett, P. C., Webster, R. L., Harding, M. E., Jedrzejewski, R. I., Foltz, C. B., Chaffee, F. H., Irwin, M. J., & Le Fèvre, O. 1989, ApJ, 346, L61
Irwin, M. J. 1985, MNRAS, 214, 575
Irwin, M. J., & Hall, P. 1982, Occas. Rep. R. Obs. Edinburgh, 10, 111
Keeton, C., & Kochanek, C. S. 1996, in IAU Symp. 173, Astrophysical Applications of Gravitational Lensing, ed. C. S. Kochanek & J. N. Hewitt (Dordrecht: Kluwer), 419
Kochanek, C. S. 1995, ApJ, 453, 545
Landolt, A. U. 1983, AJ, 88, 439
———. 1992, AJ, 104, 340
McLeod, B. A., Bernstein, G. M., Rieke, M. J., Tollestrup, E. V., & Fazio, G. G. 1995, ApJS, 96, 117
McLeod, B. A., & Rieke, M. J. 1995, ApJ, 454, 611
Metcalfe, N., Shanks, T., Fong, R., & Roche, N. 1995, MNRAS, 273, 257
Morris, S. L., Weymann, R. J., Anderson, S. F., Hewett, P. C., Foltz, C. B., Chaffee, F. H., & Francis, P. J. 1991, AJ, 102, 1627
Postman, M., Lubin, L. M., Gunn, J. E., Oke, J. B., Hoessel, J. G., Schneider, D. P., & Christensen, J. A. 1996, AJ, 111, 615
Schneider, P., Ehlers, J., & Falco, E. E. 1992, Gravitational Lenses (Berlin: Springer)
Songaila, A., Cowie, L. L., Hu, E. M., & Gardner, J. P. 1994, ApJS, 94, 461
Surdej, J., Remy, M., Smette, A., Claeskens, J.-F., Magain, P., Refsdal, S., Swings, J.-P., & Véron-Cetty, M. 1993, in Gravitational Lenses in the Universe, ed J. Surdej, D. Fraipont-Caro, E. Gosset, S. Refsdal, & M. Remy (Liège: Univ. Liège), 153
Wampler, E. J. 1997, ApJ, 476, L55
Zabludoff, A. I., Huchra, J. P., & Geller, M. J. 1990, ApJS, 74, 1